Aerodynamic Behavior of a Compound Wing Configuration in Ground Effect

Saeed Jamei, Ad. Maimun, Shuhaim. Mansor, Agoe. Priyanto, No. Azwadi
Department of Marine Technology Faculty of Mechanical Engineering
Universiti Teknologi Malaysia, UTM Skudai, Johor
jsaeed2@live.utm.my

ABSTRACT

The aerodynamic coefficients of wing in ground effect can be affected with its design which can be the main parameter for efficiency of wing-in-ground effect craft. In this study, the aerodynamic coefficients of a compound wing were numerically determined in ground effect. The compound wing was divided into three parts with one rectangular wing in the middle and two reverse taper wings with an anhedral angle at the sides. An NACA6409 airfoil was employed as a section of wings. Three dimensional (3D) computational fluid dynamics (CFD) was applied as a numerical scheme. A realizable *k-ε* turbulent model was used for simulation the turbulent flow around the wing surfaces. For validation purpose, the numerical results of a compound wing with aspect ratio 1.25, at ground clearance of 0.15 and different angles of attack were compared with the current experimental data. Then, the aerodynamic coefficients of the compound wings were computed at various ground clearances and angle of attack of 4°. According to pressure and velocity distribution of air around wing surfaces, ground clearance had considerable effects on ram effect pressure and tip vortex of compound wing, and aerodynamic coefficients of compound wing had some improvements as compared with rectangular wing.

Keywords: Aerodynamic coefficients; CFD simulation; Compound wing; Wind tunnel, Wing-in-ground effect.

NOMENCLATURE

a Anhedral angle
b Wing Span
b_m Middle wing span
c Chord length
C_D Drag Coefficient
C_L Lift Coefficient
c_t Tip chord length
D Drag Force
G_b Generation of turbulence kinetic energy due to buoyancy
G_k Generation of turbulence kinetic energy due to the mean velocity gradients
h Height of trailing edge above the ground
h/c Ground clearance
k Turbulent kinetic energy
L Lift force
L/D Lift to drag ratio
S Wing planform area
S_{ij} Mean rate of deformation tensor
U Free stream mean velocity
u_j Velocity in jth direction
Y_M Effects of compressibility on turbulence
α Angle of attack
ε Turbulent energy dissipation rate
λ Taper ratio (c/c_t)
μ Air viscosity
μ_t Turbulent viscosity
ρ Air density

INTRODUCTION

Recently, many countries started to work on WIG crafts and developed because of their advantages such as fuel saving, high speed compared to other water vehicles transport. The study on configuration of WIG crafts experimentally and theoretically is investigated to improve their aerodynamic performance. The principal means to develop lifting force is the ram effect; lift is improved when flow underneath the wing body around stagnation point on the pressure surface (lower surface of body) is trapped. The gathering of high pressure on lower surface and low pressure on upper surface of the body provides a high lifting force which is increased the source of supporting.

Two phenomena influence on aerodynamic characters of wing when a wing approaches to the ground. These are called span dominated and chord dominated ground effect. The main parameter related to span dominated ground effect is h/b (height-to-span ratio) and for chord dominated ground effect is h/c (height-to-chord ratio). The span dominated ground effect causes a reduction in drag force. There are two main source drags for aircraft which are called the viscous drag and induced drag. The viscous drag is created by friction between the air and surface of the aircraft; hence it depends on wetted area. The induced drag is related to generation of lift. Positive lift is generated when the static pressure on pressure side (lower surface) is greater than that on suction side (upper surface) of wing. The higher pressure on lower surface meets the lower pressure on upper surface at the tip of wing, subsequently around the wingtip; a current of the air will appear from lower surface to the upper surface that is called tip vortex. This vortex takes energy from aircraft; therefore it defines as a drag. The aspect ratio of wing affects on tip vortex, for high aspect ratio wing the difference between pressure on upper and lower surfaces is lower at wingtip then the tip vortex is weaker and consequently induced drag is smaller. When the wing is near the ground the tip vortex is trapped by the ground and reduces the strength of vortices, it seems that the effective aspect ratio of the wing is greater than geometric aspect ratio (Abramowski, 20071).

The chord dominated ground effect mostly can increase lift force. When the wing approaches to the ground, a higher pressure (ram effect) is generated at lower surface of the wing that is called dynamic air cushion. For very low ground clearance (h/c) the air flow reaches to stagnate accordingly the highest pressure is appear at lower surface of the wing. At small ground clearance and very small or negative angle of attack, When the lower surface of wing is convex a suction effect is created at bottom and pulled down the wing. This outcome can use for design of race car to control it at high speed. Normally, the wing of WIG crafts should have as flat as possible and positive of angle of attack (Abramowski, 20071).

Several initial experimental and computational techniques to calculate the lift by special shape of the body in ground proximity can be found in the references [Davis and Harris, 1973; Barrows, 1973; Widnall and Barrows, 1970).Yang et al. (2010) worked on longitudinal stability of WIG craft respect to some design parameters such as wing section, wing plan form, stabilizer, and endplate. They showed that the s-shaped wing modifies longitudinal stability at certain angle of attack but lost a little lift compared to popular wing section like Clark-y. Also, they depicted a tail wing more effect on centre in pitch than centre in height, because the tail position was out of ground effect. It was shown the aerodynamic centres of forward swept (FS) wing and reversed forward swept (RFS) wing is nearer to leading edge of wings contrast to rectangular wing one. The performance (L/D) of rectangular wing was lower RFS wing and greater than FS wing in extreme ground effect. The canard wing as a replacement for tail wing is an alternative design parameter for stability of WIG craft (Li, Yang and Yang, 2010a-b). Li et al. (2010b) showed that the canard wing causes the aerodynamic centres shift to leading edge of main wing without changing the relationship between centres. This is an advantage for locating the centre of gravity. The weak point of canard wing was reported on its height stability, although it has good behaviour on pitching stability. They established the drag force of canard wing is lesser than tail wing that gives higher efficiency. Lee et al. (2010) carried out the aerodynamic characteristics of rectangular wing with anhedral angle and endplates respect to different angles of attack and ground clearances. Three configurations were examined, clean wing, wing with endplate and wing with anhedral angle. The lift to drag ratio of wing with anhedral angle was in the middle among them, additionally, its height static stability satisfied for all angle of attacks and ground clearances. They described that the variations of lift coefficient of wing with anhedral angle versus Reynolds numbers is the smallest, while for drag coefficient is the largest compared to other models. The planform of wing is a new challenge in design of WIG craft (Yang and Yang, 2009; Ying et al., 2010). Yang and Yang (2009) numerically analyzed two configurations of WIG craft, one with airplane concept and another with Lippisch concept. The main wing of airplane type was rectangular wing, and the reverse forward swept wing was used for the Lippisch type. They found that the performance and stability of the Lippisch type WIG craft was better airplane type. The higher lift coefficient and lower drag coefficient were found for the Lippisch type at different ground clearance and angle of attack. The Lippisch type WIG craft can fly in and out of ground effect with acceptable height static stability.

This study tries to show the aerodynamic coefficients of a new compound wing configuration in ground effect. This compound wing is composed of three parts; a rectangular wing in the middle and two reverse taper wings with an anhedral angle at the sides. Lift and drag coefficients, lift to drag ratio, moment coefficient and centre of pressure of the present compound wing were measured respect ground clearances and Reynolds numbers. The numerical simulation employed a three dimensional CFD using a finite volume scheme. A realizable *k-ε* turbulent model was used for the turbulent flow around the wing. The aerodynamics forces were experimentally measured in the low speed wind tunnel at the Universiti Teknologi Malaysia (UTM-LST).

CFD NUMERICAL STUDY

Present numerical study was carried out by a model of rectangular wing and some compound wings with NACA6409 airfoil section. The principal dimensions of wings (Fig. 1) are shown in Table 1. These simulation were prepared with respect to different angle of attack and ground clearance (h/c), aspect ratio 1.25 and velocity of airflow 25.5 m/s. Ground level (h) is defined by the distance between trailing edge of wings centre and ground surface. The numerical scheme considered a steady –state, incompressible by means of realizable *k-ε* turbulent model of the Navier-stokes equations for flow over wing surface. The CFD models applied Fluent software and high speed computer. The transport equations for the turbulent kinetic energy (*k*) and turbulent dissipation energy (*ε*) are expressed as follows.

$$\frac{\partial}{\partial t}(\rho k)+\frac{\partial}{\partial x_j}(\rho k u_j)=\frac{\partial}{\partial x_j}\left[\left(\mu+\frac{\mu_t}{\sigma_k}\right)\frac{\partial k}{\partial x_j}\right]+G_k+G_b-\rho\varepsilon-Y_M+S_k \quad (1)$$

and

$$\frac{\partial}{\partial t}(\rho \varepsilon)+\frac{\partial}{\partial x_j}(\rho \varepsilon u_j)=\frac{\partial}{\partial x_j}\left[\left(\mu+\frac{\mu_t}{\sigma_\varepsilon}\right)\frac{\partial \varepsilon}{\partial x_j}\right]+\rho C_1 S\varepsilon-\rho C_2\frac{\varepsilon^2}{k+\sqrt{\nu\varepsilon}} \quad (2)$$

$$+C_{1\varepsilon}\frac{\varepsilon}{k}C_{3\varepsilon}G_b+S_\varepsilon$$

$$C_1=\max\left[0.43,\frac{\eta}{\eta+5}\right],\eta=\frac{k}{\varepsilon},S=\sqrt{2S_{ij}S_{ij}} \quad (3)$$

where S_k and S_ε are user-defined Source terms, $C_{1\varepsilon}$, C_2, $C_{3\varepsilon}$, σ_k and σ_ε are the adaptable constants.
The aerodynamic coefficients and centre of pressure in this numerical study were determined as follows:

$$C_L=\frac{L}{0.5\rho U^2 A}, C_D=\frac{D}{0.5\rho U^2 A}, C_M=\frac{M}{0.5\rho U^2 Ac}$$

and $X_{CP}=0.25+\dfrac{C_M}{C_L\cos\alpha+C_D\sin\alpha}$.

(a)

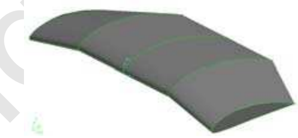

(b)

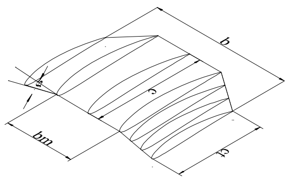

(c)

Fig. 1. Types of wing configuration, (a) Rectangular wing, (b) Compound wing, (c) Geometry of the compound wing.

Table 1. Principal dimension of rectangular wing and compound wings with different middle wing span.

Dimension	Rectangular wing	Compound wing-1
Total wing span (b)	250 mm	250 mm
Root chord length (c)	200 mm	200 mm
Middle wing span (b_m)	-	125
Taper ratio (c/c_t)		1.25
Anhedral angle (a)		13°

EXPERIMENTAL PROCEDURES AND SET-UP

In the wind tunnel, aerodynamic force measurements were carried out at ground clearances (h/c) and different angles of attacks (α). Ground clearance (h/c) was defined as the distance ratio between the wing trailing edge center and ground surface (h) to root chord length (c) of the wing. The range of the angles of attacks are small because of limitations, such as touching wing to ground and certain test procedures for some ground clearances. Fig. 2 shows the experimental setup of current experiment in the low speed wind tunnel at the Universiti Teknologi Malaysia (UTM-LST).

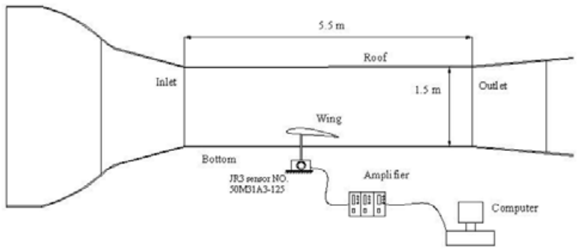

Fig. 2. Experimental setup in the low speed wind tunnel at the Universiti Teknologi Malaysia.

TENDENCY OF NUMERICAL AND EXPERIMENTAL SIMULATIONS

In this project, according to numerical and experimental simulations it can be seen that the results of both simulations have similar trend. Fig. 3a-b shows the aerodynamic coefficients of rectangular and compound wings at ground clearance of 0.15. The numerical results had some deviations from experiments but both simulations show the compound wings have some improvements in aerodynamic performance compared to rectangular wing at small ground clearance (h/c ≤0.2). Both simulations confirmed that drag coefficient of compound wing was smaller than rectangular wing one at small ground clearance and angle of attack greater than 2°, and lift to drag ratio of compound wing was greater than rectangular wing one as well. It is important that the experiments validated the performance of compound wing where there are some improvements at low ground clearances. In validation purpose, the experimental results confirmed the compound wing is suitable configuration to employ in WIG crafts to fly near the ground.

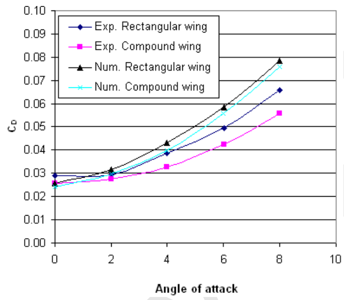

(a) Drag coefficient

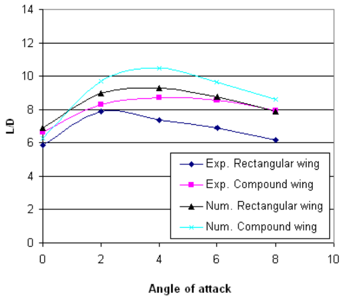

(b) Lift to drag ratio

Fig. 3. Comparison of experimental and numerical simulation results at ground clearance of 0.15, (a) Drag coefficient, (b) Lift to drag ratio.

RESULTS AND DISCUSSIONS

Pressure and velocity contours

Figs. 4-9 show the pressure and velocity distribution of compound wing-1 (Table 1) at ground clearances of 0.1 and 0.4 with angle of attack of 4°. Fig. 4 demonstrates the suction effect on the upper surface of compound wing-1 at ground clearance of 0.1 is slightly stronger. There is a higher pressure near leading edge of upper surface at ground clearance of 0.4 that means the stagnation point is nearer to leading edge at this height. The higher pressure distribution on lower surface of compound wing-1 shows the pressure increased in lower side of the compound wing at ground clearance of 0.1. At lower ground clearance, there is higher pressure in flow passage between lower side of compound wing-1 and ground at middle span as shown in Figs. 5-6, also the stagnation point moves to lower side of compound wing-1 as wing approaches to ground. Figs. 7-8 depict higher velocity in flow passage under compound wing-1 at ground clearance of 0.4. The pressure distribution near wingtip of compound wing-1 at ground clearance of 0.1 indicates that its tip vortices are gradual weaker compared to higher ground clearance (Fig. 9), therefore, the induced drag of compound wing drops when ground clearance is decreased.

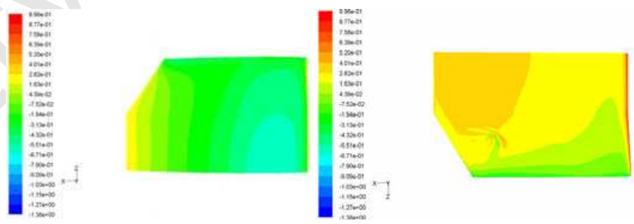

Upper surface Lower surface

(a) Compound wing-1 (h/c=0.1)

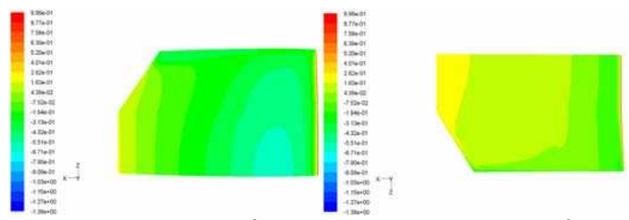

Upper surface Lower surface

(b) Compound wing-1 (h/c=0.4)

Fig. 4. Pressure coefficient contour on upper and lower surface of compound wing-1 at ground clearances of 0.1 and 0.4 with angle of attack of 4°.

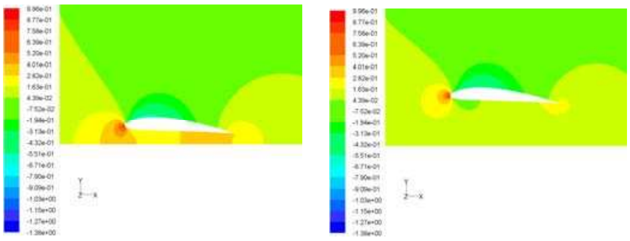

(a)Compound wing-1 (h/c=0.1)   (b) Compound wing-1 (h/c=0.4)

Fig. 5. Pressure coefficient contour on the middle span of compound wing-1 at ground clearances of 0.1 and 0.4 with angle of attack of 4°.

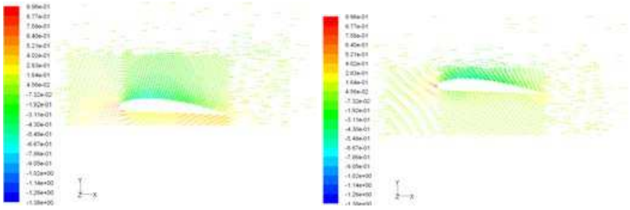

(a) Compound wing-1 (h/c=0.1)   (b) Compound wing-1 (h/c=0.4)

Fig. 6. Velocity vector colored by pressure coefficient on the middle span of compound wing-1 at ground clearances of 0.1 and 0.4 with angle of attack of 4°.

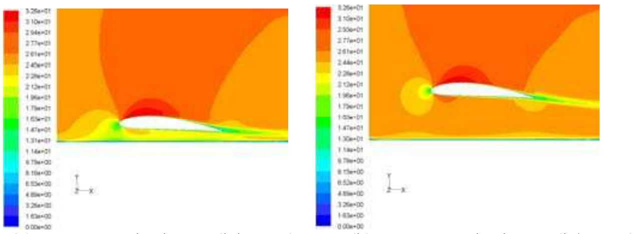

(a) Compound wing-1 (h/c=0.1)   (b) Compound wing-1 (h/c=0.4)

Fig. 7. Velocity contour (m/s) on the middle span of compound wing-1 at ground clearances of 0.1 and 0.4 with angle of attack of 4°.

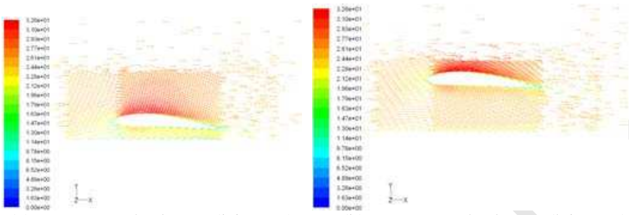

(a) Compound wing-1 (h/c=0.1)   (b) Compound wing-1 (h/c=0.4)

Fig. 8. Velocity vector colored by velocity magnitude (m/s) on the middle span of compound wing-1 at ground clearances of 0.1 and 0.4 with angle of attack of 4°.

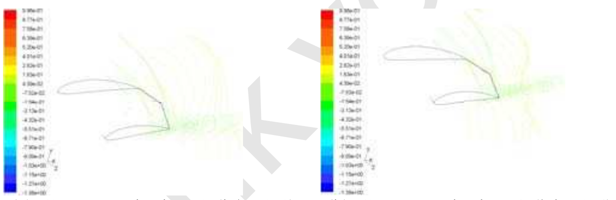

(a) Compound wing-1 (h/c=0.1)   (b) Compound wing-1 (h/c=0.4)

Fig. 9. Pressure coefficient distribution near wingtip of compound wing-1 at ground clearances of 0.1and 0.4 with angle of attack of 4°.

Lift coefficient

The effect of different ground clearance on aerodynamic coefficients of rectangular wing and compound wing-1 (Table 1) at angle of attack of 4° is shown in Tables 2-6 and Figs. 10-14. Fig. 10 illustrates quick increase in the lift coefficients of both wings as ground clearance was decreased specially at ground clearance lesser than of 0.2 compound wing-1 has a favorable enhancement where the plot of lift coefficient of compound wing-1 is upper than rectangular wing ones. According to the present results the decreasing of ground clearance could improve considerably the ram pressure on lower surface of compound wing-1. The increment of lift coefficient of compound wing-1 compared with rectangular wing was calculated by Eq. 4 and summarized in Table 2. The increments have substantial value at small ground clearance where at ground clearance of 0.1 is 17.3 percent.

$$Increment(\%) = \frac{C_{L(Compound)}}{C_{L(\mathrm{Rec\,tan\,gular})}} - 1 \tag{4}$$

Table 2. Lift coefficient and its increment versus ground clearance at angle of attack of 4° for rectangular wing and compound wing-1.

Ground clearance	Lift coefficient		Increment of C_L (%)
	Rectangular wing	Compound wing-1	
0.1	0.428	0.502	17.3
0.15	0.400	0.416	4.0
0.2	0.384	0.385	0.4
0.3	0.364	0.353	-3.0
0.4	0.352	0.337	-4.2

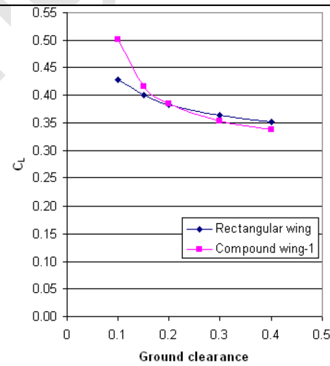

Fig. 10. Lift coefficient (C_L) versus ground clearance at angle of attack of 4°.

Drag coefficient

The drag coefficients of rectangular wing and compound wing-1 (Table 1) versus ground clearance are depicted in Fig. 11; in addition the reduction of drag coefficient of compound wing-1 was calculated by Eq. 5 in Table 3. Fig. 11 reveals a small variation in the drag coefficient of both wing with increase ground clearance while the plot of compound wing-1 is sizable lower than rectangular wing one. The weaker tip vortex of compound wing-1 is main reason of the reduction in its drag coefficient compared to rectangular wing. As mentioned before, smaller ground level and area of the tip of compound wing-1 causes weaker tip vortex. The reduction of drag coefficient is between 5.9-8.6 percent as shown in Table 3.

$$Reduction(\%) = 1 - \frac{C_{D(Compound)}}{C_{D(Rectangular)}} \quad (5)$$

Table 3. Drag coefficient and its reduction versus ground clearance at angle of attack of 4º for rectangular wing and compound wing-1.

Ground clearance	Drag coefficient		Reduction of C_D (%)
	Rectangular wing	Compound wing-1	
0.1	0.0430	0.0405	5.9
0.15	0.0430	0.0397	7.8
0.2	0.0430	0.0400	6.8
0.3	0.0432	0.0395	8.6
0.4	0.0433	0.0407	6.0

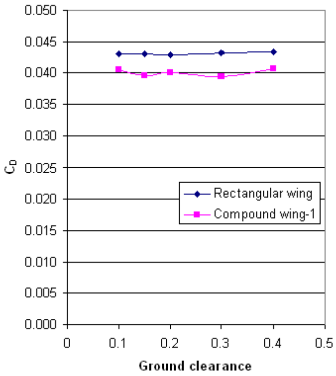

Fig. 11. Drag coefficient (C_D) versus ground clearance at angle of attack of 4°.

Lift to drag ratio

The lift to drag ratio of rectangular wing and compound wing-1 (Table 1) versus ground clearance was summarized in Table 4, in addition, the increment of lift to drag ratio of compound wing-1 was determined by Eq. 6. The increment of lift to drag ratio of compound wing-1 is noticeable at all ground clearance especially at low ground clearance, for example, at ground clearance of 0.1, this increment is 24.7 percent. The trend of lift to drag ratio of compound wing-1 and rectangular wing versus ground clearance is shown in Fig. 12.

$$Increment(\%) = \frac{L/D_{(Compound)}}{L/D_{(Rectangular))}} - 1 \quad (6)$$

Table 4. Lift to drag ratio and its increment versus ground clearance at angle of attack of 4º for rectangular wing and compound wing-1.

Ground clearance	Lift to drag ratio		Increment of L/D (%)
	Rectangular wing	Compound wing-1	
0.1	9.93	12.39	24.7
0.15	9.29	10.48	12.8
0.2	8.93	9.63	7.8
0.3	8.42	8.94	6.2
0.4	8.13	8.29	1.9

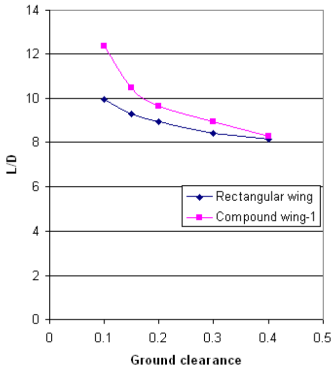

Fig. 12. Lift to drag ratio (L/D) versus ground clearance at angle of attack of 4°.

Moment coefficient and centre of pressure

The variation of moment coefficients of rectangular wing and compound wing-1 (Table 1) versus ground clearance is shown in Table 5 and Fig. 13. A moment coefficient that causes a decreasing on angle of attack was defined as a positive moment. The trend of moment coefficients in Fig. 13 indicates the increasing of ground clearance causes a drop in moment coefficient and stability of compound wing-1 and rectangular wing, although the rate of this decline is higher for compound wing-1. The reduction of moment coefficient of compound wing-1 was calculated by Eq. 7 in Table 5. This reduction is small at low ground clearance where it is 3.2 percent at ground clearance of 0.1, however, it increases rapidly by raising the ground clearance. In Table 6, the reduction of distance of center of pressure from leading edge of compound wing-1 was calculated by Eq. 8, this reduction is between 7-8 percent. Based on present results the moving of the center of pressure of compound wing-1 and rectangular wing is small with respect to variation of ground clearance as shown in Fig. 14.

$$Increment(\%) = 1 - \frac{C_{M(Compound)}}{C_{M(Rectangular)}} \quad (7)$$

$$Reduction(\%) = 1 - \frac{X_{CP}/c_{(Compound)}}{X_{CP}/c_{(Rectangular)}} \quad (8)$$

Table 5. Moment coefficient and its reduction versus ground clearance at angle of attack of 4º for rectangular wing and compound wing-1.

Ground clearance	Moment coefficient		Reduction of C_M (%)
	Rectangular wing	Compound wing-1	
0.1	0.075	0.073	3.2
0.15	0.072	0.061	15.9
0.2	0.069	0.057	18.2
0.3	0.065	0.052	20.6
0.4	0.060	0.047	21.0

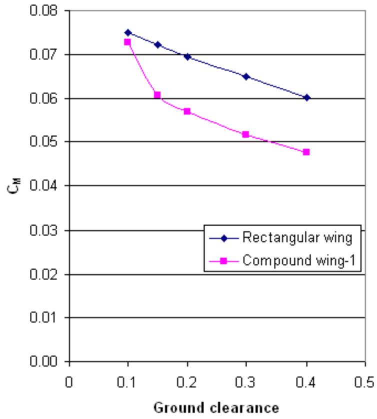

Fig. 13. Moment coefficient (C_M) versus ground clearance at angle of attack of 4°.

Table 6. Centre of pressure and its reduction versus ground clearance at angle of attack of 4º for rectangular wing and compound wing-1.

Ground clearance	Centre of pressure		Reduction of X_{CP}/c (%)
	Rectangular wing	Compound wing-1	
0.1	0.425	0.394	7.2
0.15	0.430	0.395	8.0
0.2	0.430	0.397	7.7
0.3	0.427	0.395	7.5
0.4	0.419	0.390	7.1

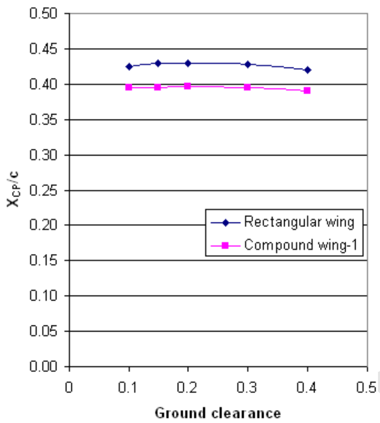

Fig. 14. Centre of pressure (X_{CP}/c) versus ground clearance at angle of attack of 4°.

CONCLUSION

The aerodynamic characteristics of a compound wing were numerically investigated. The compound wing is divided into three parts; the middle part as the rectangular wing and two side parts that are reverse taper wing with an anhedral angle. The excellent performance of compound wing was in small ground clearance (h/c< 0.2). There was favorable increment of the lift coefficient in small ground clearance, although, drag coefficient had no more variation with ground clearance but lift to drag ratio of compound wing had substantial improvement. At small ground clearance, there was high ram effect and low tip vortex for compound wing compared to rectangular wing. The reduction of moment coefficient of compound wing was faster than rectangular wing one as ground clearance of wings was decreased. Also, the percentage of this reduction was high for compound wing. Meanwhile, the position of centre of pressure of both compound and rectangular wings had small fluctuation. The center of pressure of compound wing compared to rectangular wing is nearer to leading edge.

ACKNOWLEDGEMENTS
The authors would like to thank the Ministry of Science, Technology, and Innovation (MOSTI) Malaysia for funding this research.

REFERENCES

Abramowski, T (2007). "Numerical investigation of airfoil in ground proximity," *Journal of Theoretical and Applied Mechanics*, Vol. 45, No. 2, pp. 425-436.

Barrows, TM (1973). "The ram air cushion-advanced fluid suspension for tracked levitated vehicles," *ASME 73-ICT-14*.

Davis, JE, and Harris GL (1973). "Nonplanar wings in nonplanar ground effect," *Journal of Aircraft*, Vol. 10, No. 5, pp. 308-312.

Lee, J, Han, CS, and Bae, CH (2010). "Influence of wing configurations on aerodynamic characteristics of wings in ground effect," *Journal of Aircraft*, Vol. 47, No. 3, pp. 1030-1040.

Li, Y, Yang, W, and Yang, Z (2010a). "Numerical Study on wing in ground effect of canard configuration," *Aeronautical Computing Technique*, Vol. 40, No.4, pp. 27-30.

Li, Y, Yang, W, and Yang, Z (2010b). "Numerical study on static longitudinal stability of canard WIG Craft," *Flight Dynamics*, Vol. 28, No. 1, pp. 9-12.

Widnall, SE, and Barrows, TM (1970). "An analytic solution for two and three-dimensional wings in ground effect," *Journal of Fluid Mechanics*, Vol. 41, No. 4, pp. 769-792.

Yang, W, and Yang, Z (2009). "Aerodynamic investigation of a 2D wing and flows in ground effect," *Chinese Journal of Computational Physics*, Vol. 26, No. 2, pp.231-240.

Yang, W, Yang, Z, and Ying, C (2010). "Effects of design parameters on longitudinal static stability for WIG craft," *International journal of Aerodynamics*, Vol. 1, No. 1, pp. 97-113.

Ying, C, Yang, W, and Yang, Z (2010). Numerical simulation on reverse forward swept wing in ground effect," *Computer Aided Engineering*, Vol. 19, No. 3, pp. 35-39.